



# EXAMINATION OF ARTIFICIAL INTELLIGENCE IN IMAGE PROCESSING DEPLOYING DEEP LEARNING TO IDENTIFY ABNORMAL PHYSIOLOGICAL CONDITIONS FROM CHEST XRAY

<sup>1</sup>Utsab Ray, <sup>2</sup>Jayanta Mallick, <sup>3</sup>Karabi Ganguly, <sup>4</sup>Sandip Bag, <sup>5</sup>Sabyasachi Sen

<sup>1</sup>BTech, Department of Biomedical Engineering, <sup>2</sup>BTech, Department of Biomedical Engineering,

<sup>3</sup>Associate Professor and HOD, Department of Biomedical Engineering

<sup>4</sup>Associate Professor, Department of Biomedical Engineering

<sup>5</sup>Associate Professor and HOD, Department of Physics

<sup>1</sup>Department of Biomedical Engineering,

<sup>1</sup>JIS College of Engineering, Kalyani, Nadia, India

**Abstract :** The study of thoracic diseases and their classification has been one of the most fascinating research subjects in recent years. The quantity of medical picture collections is expanding quickly in to document diseases in hospital due to the different implementations of clinical graphics in medical institutions, pathology, and diagnostic centres. Despite that fact that there have been many studies on this topic, this area is still complex and challenging. The publications did use a variety of classification methods for their medical content. The main drawback of conventional approaches is indeed the semantic gap among high-level corpora observed by people and medical imaging devices' restricted participants expressed. The comprehensive CNN model neuronal network is a new technique that was developed as a result of the challenges associated with processing and querying enormous datasets. Recently, machine vision or medical engineering have benefited greatly from deep learning techniques. In this study, we proposed and examined a robust, fully-connected cognitive intranet for identifying chest diseases. The suggested model consists of pooling, Densenet 121, convolutional, and fully connected layers. There are fifteen output units in the last fully connected layer. One of fifteen disorders will be predicted by each transmitter. A publicly accessible dataset named Chest X-Ray 8 was utilized to train this model. It contains fifteen categories with corresponding labelling but no finding images. The performance of this model in multiclass classification is surprising. The comparative study shows how effective the suggested model is in terms of the ROC curve. For categorising classification digital records for diverse thoracic disorders, the suggested approach is very appropriate.

**Keywords - thoracic, CNN, DenseNet 121, diseases, chest x-ray, ROC Curve, classification.**

## I. INTRODUCTION

According to WHO estimation, 8.8 million individuals died of cancer as their initial cause in 2015 [1]. 1.69 million of these fatalities, or close to 20%, were caused by lung cancer [1]. While early detection makes for the most effective treatment, the screening programme is crucial in preventative care. This study found that lobulation, anisotropic dissipation, or a pleomorphic silhouette are more frequently seen in malignant lung nodules [2].

Lung cancer screening now frequently employs lower dose computed tomography (LDCT) [3]. The use of LDCT vetting has been noticed for patients with high-risk demographics and has facilitated cancer cases [3]. Standard dosage CT imaging (CT) can be used to monitor the outcome of LDCT screening [4]. However, there are many obstacles to the application of LDCT screening, including providers' worries about connections to LDCT machines and the cost to rural residents [3]. Rural residents also have restricted access to specialists and primary care doctors [3]. On the other hand, chest x-rays are routinely available in rural areas. However, chest x-rays produce lower local quality images than LDCT or CT scans, therefore a lower quality diagnosis is assumed.

The goal of this study is to determine whether using chest x-rays along with the principal computer assessment (CADx) method can improve the accuracy of emphysema diagnoses.

The convolutional neural network (CNN) has demonstrated excellent performance in picture classification and identification tasks. LeNet [5, AlexNet [6, ZDNet [7, VGG [8, Inception [9], Inception-ResNet [12], DenseNet [14], Xception [13], NASNet [15], and

ResNet [11] are the first networks developed by CNN. Convolutional networks have been used in numerous research to detect apparent confusion in chest x-rays. M. T. Islam et al. [16] use several cnns group application to discover deficiencies in chest x-rays. Research on the application of CNNs to identify thoracolumbar disorders from radiographic images was also done by X. Wang et al.

They, too, used a sizable dataset for their research [17]. Many studies, like ChexNet [18] and the Attention Guided Pcn (AG-CNN) [19], on the implementation of High Redundancy Convolutional Networks (DenseNet) [14] to detect thoracic diseases are now being done. In both cases, the neural network is trained using a sizable sample of chest x-ray pictures.

The tiny sample size is a concern when attempting to forecast lung cancer using CNN. On a sizable image dataset, CNN offers a multitude of options that can be changed. With ImageNet, a common picture dataset with more than one million images, scientists routinely train CNN models in practise. After that, even a dataset of extremely particular images is repaired by the experienced CNNs. Sadly, the accessible melanoma picture library is too small, also with data augmentation, for with this transfer learning to be successful. The concept of employing transfer learning to progressively enhance the model's performance has been put forth multiple times as a solution to this problem. In this paper, transfer learning is employed twice. The foundation for lung cancer were moved once the model had been moved from the grayscale to the chest x field. Second, the lung cancer framework will be transferred. Such inter knowledge can get beyond the problem of a small sample size and produce a greater task lead when compared to the standard transfer learning technique. This study also shows how the model may be altered to understand a heat map showing the anticipated perspective of fibrosis similar to a chest x-ray profile.

Medical picture sets have increased dramatically in recent years as a result of technological advancements, image analysis, and image-based research. The digitalisation processing and data storage system has benefits for medical treatments and research analysis. A variety of hospitals and diagnostic facilities provide a lot of data. A detailed investigation of the ailments is therefore a challenging undertaking. Several approaches had been put out for the analysis of these substantial data sets. Deep learning-based categorization is one of the most efficient methods for finding medical information. Deep-learning algorithms can generate solutions that are nearly optimal in terms of practicality cos of their end-to-end adaptability. A survey found that methods using deep learning can address a variety of crucial issues in the actual world [20,24].

Thoracic diseases still come in more than 200 different varieties. They are frequently frightful, such emphysema, fibrosis, and fibroid. These illnesses make it harder for the body to breathe and circulate blood. And over 15% of the society is impacted by these disorders, according to various research. However, in some instances, it might be challenging to distinguish pictures from reduced, smooth, and low-resolution images. However it is challenging to diagnose many illnesses in their initial stages with normal symptoms. To address this issue, we turned to a brand-new, sizable data show called Chest X-Ray 8.

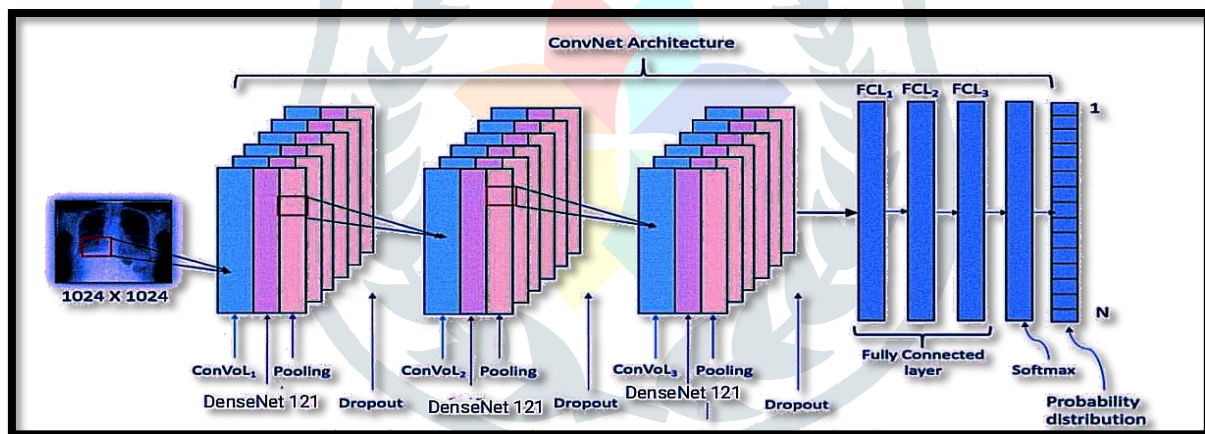


Figure (i) – Proposed Deep Learning architecture

## II. RELATED WORK

For decades, software architecture has been used to diagnose diseases. The velocity from the conventional technique to the framework of machine learning and from the machine learning approach to the deep learning prospective remain high due to its exceptional control. There are multiple methods for categorising different diseases, including gliomas, autoimmune diseases, chest infections, and many others. With combining a greater amount of datasets, the Deep Convolutional Neural Stream is among the most frequently used methods for categorising not only natural photos but also numerous sorts of medical images.

Deep Learning describes learning as the process of aiming to improve behaviour via experience. Deep learning, a branch of artificial intelligence, is used to increase productivity across a variety of machine learning application areas. High-level complexity in data is attempted to be modelled by deep architectures with many rendering units and either deterministic or stochastic flip methods [24]. Although this method was created in 1965, it has recently become more popular as a result of the speeding of GPU-based computational power and ou pas, which enables deeper networks for greater usage [25]. The use of a multi-layer activation functions with numerous hidden layers enhances the output of an artificial brain. In order to sustain neural networks, backpropagation was created in the 1980s [21].

In recent years, one of the most challenging and educational activities has been classifying digital documents. Interstitial lung diseases were also classified using Deep Learning algorithms in [26]. (ILDs). Seven illnesses, 6 of which are brought on by dead tissue, are cooperatively treated. [27] examined lung-generated CT illnesses using a constrained Boltzmann machine. They have introduced two methods for two datasets: texture identification and airway detection. [28] previously classified brain organs using a CNN network built on many kernels. In [20], a two-phase context guideline was applied, with extracted features being employed for picture classification in the first step and CNN applied to feature extraction in the second.

Convolutional Neural Network - Feed-forward neural networks with convolutional layers are primarily influenced by the human brain. Both special feature extraction and classification are possible with CNN. Four different kinds of layers are combined by CNN: Included are a fully connected layer, a weight vectors layer, a sub sampling surface, and a learning method.

A typical CNN model uses the kernel to extract feature maps from data. Data from the previous layer is received by each neuron. The performance of visual representation is enhanced by several neuron connections that are interconnected. The amount of boundaries required is reduced when weight is shared. Because each fully connected layers is connected to an original input layer, CNN can process more complex functions more quickly. It's possible that CNN occasionally overfits. Pooling is only a sub sampling technique that is usually employed to prevent over fitting and decrease the number of criteria. A networked layer or layers are then established to compile the clever features that provide the categorization outcome. In this study, we offer a sophisticated end-to-end learning approach for categorising chest illnesses. This essay also highlights CNN's range of capabilities.

The different CNN architectures are followed by different writers. In this work, we followed a simple yet fundamental architecture that was outlined in LeNet-5[30]. By changing a few filaments, kernels, cost functions, optimization methods, and hyperparameters, we trained our model. The suggested model starts with a convolutional layer that has many kernels that estimate the different features maps, then by an activation map and just a convolution. The Clustering algorithm is mostly employed to learn and comprehend more complicated functions.

The capabilities of the system should rise as the quantity of densely integrated layers increases. However, we only employ three convolutional layers in our model. The decrypted functionality of the input image are stored in the final fully connected layer. Let  $(p,q)$  represent a placement in the input vector  $x_{pq}^l$  and  $i$  is the count for feature maps of  $l^{th}$  layer. The feature map  $z_{pqi}^l$  can be calculated as

$$z_{pqi}^l = (W_i^{lT} + X_{pq}^l + s_i^l) \quad \text{----- (i)}$$

Where,  $W_i^l = \text{Weightvectors}$  ;  $s_i^l = \text{biasofeachfilterin}l^{th}\text{layer}$

Its exchange of weights in each layer gives the neural network more training power. To fathom the complex functions, the nonlinear transfer operation denoted by  $\lambda(\cdot)$  is used. The activation layer processes an input feature engendered by the convolutional layer and sends it to the pooling layer. This activation function can always be calculated and deduced as follows:

$$\lambda_{pqi}^l = \lambda(\lambda_{pqi}^l) \quad \text{---- (2)}$$

$$\lambda_{pqi}^l = \max(w_i^T X_{pq} + s_i, 0) \quad \text{---- (3)}$$

$$z_{pqi}^l = \text{pool}(\lambda_{abi}^l) \forall (a, b) \in R_{pq} \quad \text{---- (4)}$$

According to equation (4) the nearest neighbor of the respective location  $(p,q)$  is  $R_{pq}$ , the final fully connected layer is fed into such a Softmax activation layer, which gives the likelihood of the output for each class associated to the input. The result of Soft - max can be estimated as follows:

$$s_{pqi}^l = \frac{e^{z_{pqi}^l}}{\sum_{n=1}^N e^{z_{pqi}^l}} \quad \text{---- (5)}$$

One of the difficult tasks is training a neural network. Through hyper parameter training and the use of tuning sets for various parameters. The neural network's cost may be calculated as follows:

$$\delta = \frac{1}{N} \sum_{b=1}^N l(\theta; Z^{(b)}, D^{(b)}) \quad \text{----- (6)}$$

$\theta$  is the parameter set that is being used throughout the neural network,  $z^b$  symbolize the target output on CNN as output label. Adam optimizer has been deployed in this neural network.

### III. AIMS AND OBJECTIVES OF WORK

Chest x-ray images are often not dealt properly and the main problem pertaining to the images correlates the misprediction and mistreatment of thoracic disorders.

To overcome the major disorder, DenseNet 121 architecture of Deep learning has been deployed to make a deep learning model, with enhanced accuracy and effective in identification of disorders from chest xray images.

### IV. METHODOLOGY

The entire workflow succumbed a plethora of steps preceding the deep learning with the principles of image processing has been embodied in figure (ii).

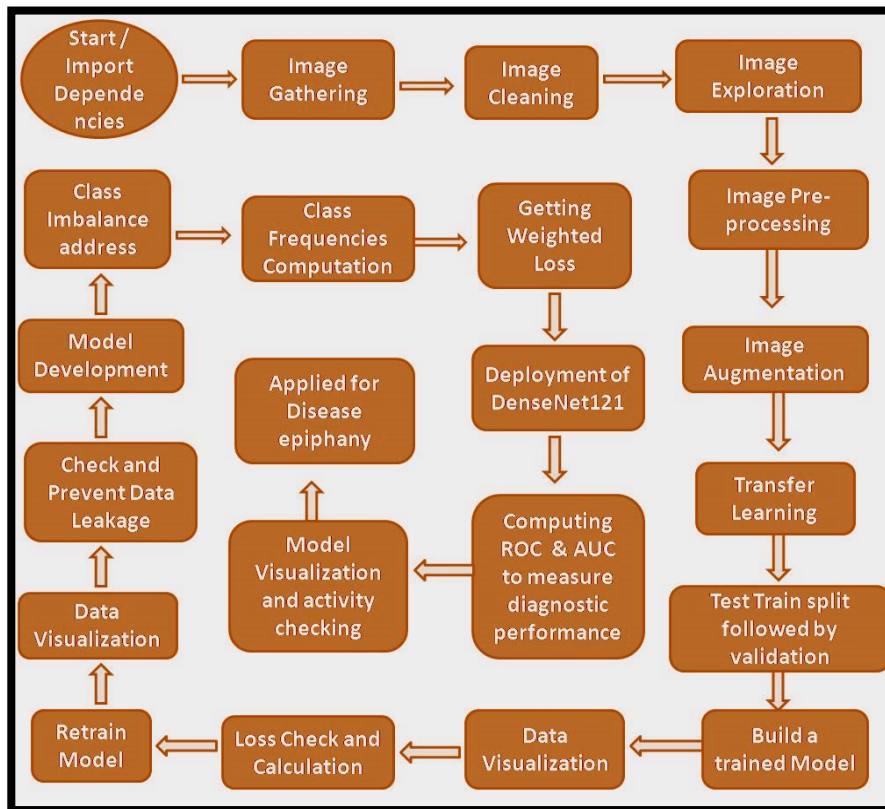


Figure (ii) – Overview of work

**Datasets** – The datasets commonly deployed in this work named as "ChestX-ray8" [31] which includes 108,948 full frontal X-ray visuals of 32,717 distinct patients with text-mined eight disease image labels (each image can have multiple labels) extracted from accompanying radiation exposure reports using natural language processing techniques.

**Data preparation** - All images were subjected to data preparation, which included the four steps outlined below as well as in figure (iii):

Step 1: Using histogram normalization, increase the juxtaposition of all images. This needs to allow the severity of images of various datasets to be normalized.

Step 2: using wiener filter with a predefined threshold of 33, remove noise from all images.

Step 3: resize images to 224x224 pixel value to match the model input used in the current study.

Step 4: Normalizing illustration color based on the ImageNet training set's mean and variance [31].

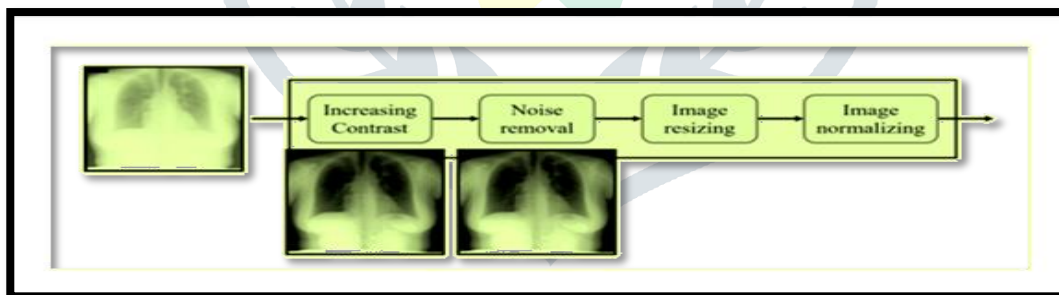


Figure (iii) – Data preparation illustration

**CNN Architecture** - The model used in this study is the 121-layer Deep Convolutional Network, which is one of several convolution neural network architectures such as Inception, ResNet, and DenseNet (DenseNet-121). This CNN has a dense block architecture, which improves data stream and resolve the vanishing gradient issue found with very deep neural systems. This CNN also outperforms many public datasets, including ImageNet. The original model takes a 224x224 pixel input image and outputs prior probability for 1,000 object classes. A last fully linked layer of the CNN has been supplanted in this work by a single sigmoid base station to output the chance of having the stipulated pathology.

**Class Imbalance** - An imbalanced classification data set is one with skewed class proportions. Majority classes are those that represent significant portions of the data set. Minority skills make up a less significant proportion of the population. The large class mismatch present in diagnostic imaging datasets is among the challenges of working with such datasets.

**Loss Function on class imbalance** - Assume we used a standard merge loss for each aetiology. We recall that the  $i$ th training data case's cross-entropy loss contribution is:

$$L_{Cross-entropy}(x_i) = -(y_i \log(f(x_i)) + (1 - y_i) \log(1 - f(x_i))),$$

where  $x_i$  and  $y_i$  are the input characteristics and the label, respectively, and  $f(x_i)$  is the model's output, i.e. the likelihood that it is favorable. It should be noted that for any training case, either  $y_i=0$  or  $(1 - y_i)=0$ , so just one of these terms pertains to the lost opportunity

The total average cross-entropy absence over the complete training set of size N can be rewritten as follows:

$$L_{Cross-entropy}(D) = -\frac{1}{N} \left( \sum_{\text{Positive Examples}} \log(f(x_i)) + \sum_{\text{Positive Examples}} 1 - \log(f(x_i)) \right)$$

We can see from this formulation that in the event of a large asymmetry with few positive test sets, for example, the loss will be monopolized by the negative class. Summing the contribution of each lesson (i.e. pathological condition) across all training cases, we recognize that the participation of each class (positive or negative) is:

$$freq_p = \frac{\text{numberofpositiveexamples}}{N}, \text{ and}$$

$$freq_n = \frac{\text{numberofnegativeexamples}}{N}$$

Transfer Learning - Transfer learning's basic premise is straightforward: take a model is trained on a huge dataset and apply its insight to a lower dimension. For object recognition, we freeze the network's early convolutional layers and therefore only train the last few pieces that make a prediction.

ROC Curve - A receiver operation characteristic curve (ROC curve) is a graph that depicts the performance of the proposed model across all classification thresholds. This graph depicts two parameters: The percentage of true positives. The Graph can be used to chose a threshold for something like a classification model that maximizes true positives while minimizing false positives. ROC Curves aid in determining the exact market between true positive rate or the false positive rate for a concept using various probability threshold measures.

Class Activation Mappings (GradCAM) - One of the difficulties with using deep learning in pharmaceuticals is that the complex architecture of neural networks makes them much more difficult to interpret than traditional machine learning models. Class Activation Maps are one of the most common methods for increasing model interpretability for computer vision tasks (CAM).

Class activation maps can help to figure how the approach is "looking" if categorizing an appearance.

## V. RESULTS AND DISCUSSIONS

For the sake of findings for thoracic disorders we proposed a new approach of detection of disorders from chest xray using datasets and the findings pertain to the main criteria of creating a framework of DenseNet 121 considering CNN model of deep learning. To conceptualize the work several test cases were undergone considering the parameters and the resultant visualization was depicted from ROC Curve and class activation mappings for increasing model interpretability.

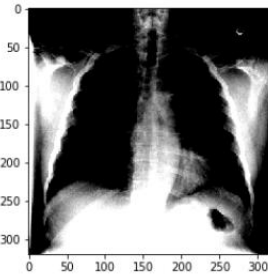


Figure (iv): Clipping input data to the imshow valid range with RGB documentation ([0..1] - floats ; [0..255] for integers). It is the data exemplified as image preparation result by eradicating away the defaults of the datasets and eliminating further leakages in images.

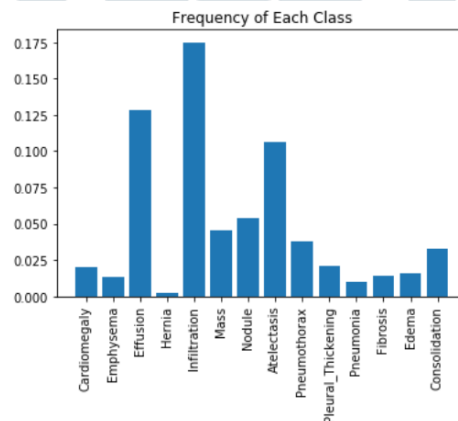


Figure (v) – Obtaining the respective diseases as class along with their respective counts as per the concerned dataset to the visualize the frequency of classes.

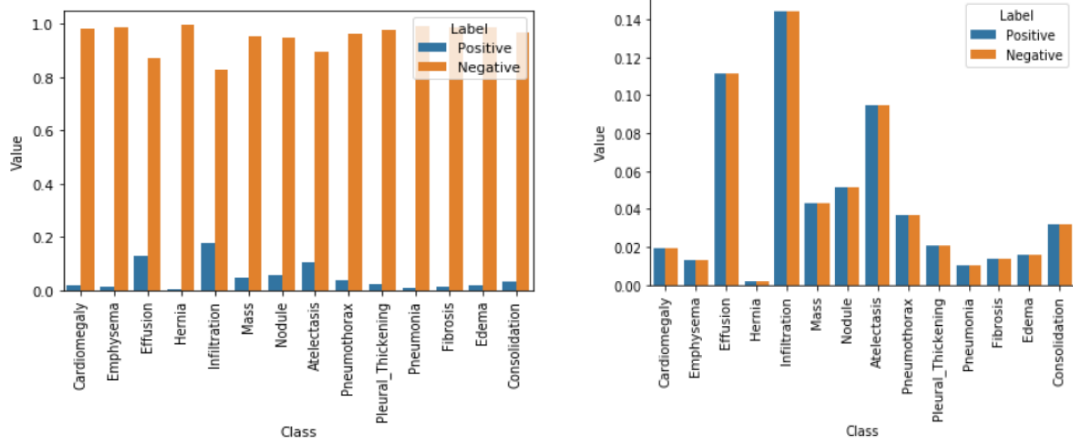


Figure (vi) and figure (vii) depicts in obtaining out the respective positive and negative cases.

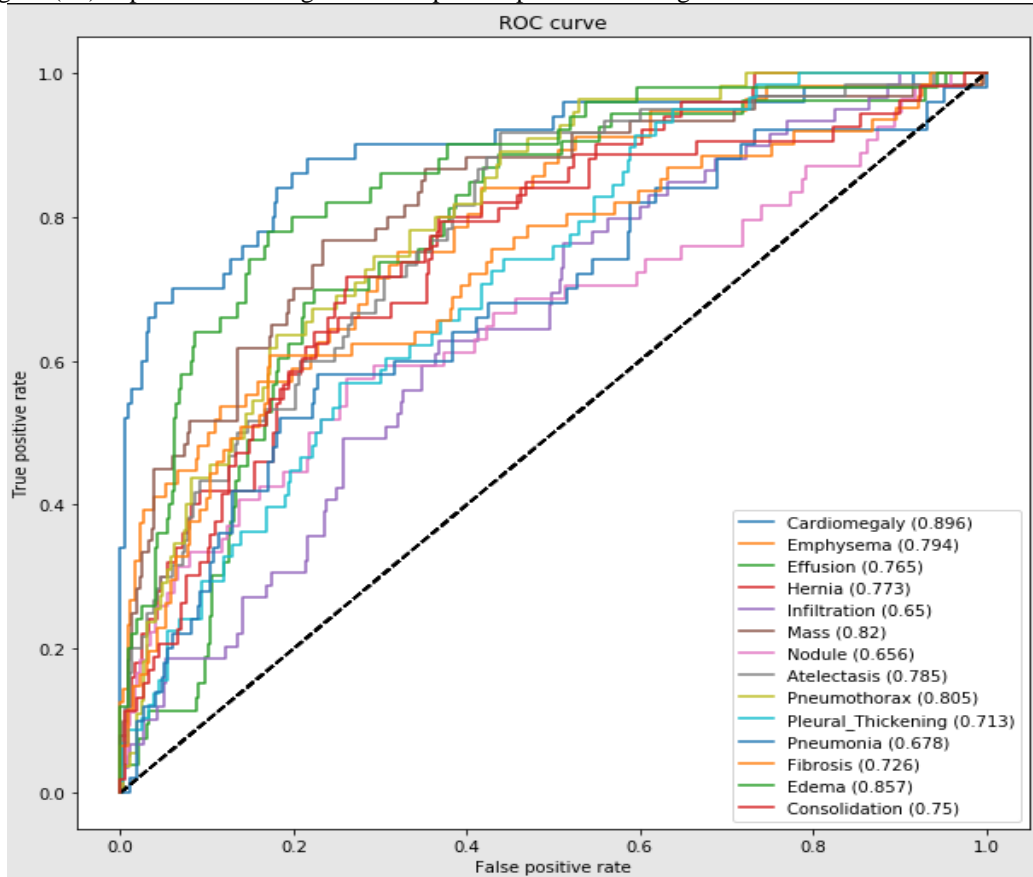


Figure (viii) to analyze, evaluate and visualize the true positive and false positive rates of the respective disorders.

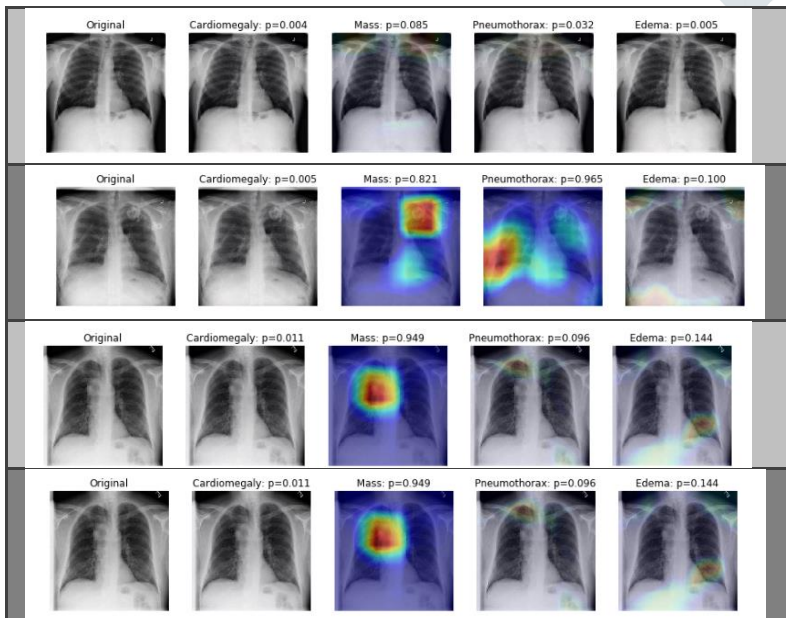


Figure (ix) represents the final visualization of disorders based on the probability rates of positive cases and region of defects using GradCAM.

## VI. CONCLUSION

From the entirety of this work, a basic conceptualization of pre-training a model from the dataset and producing a standard image for processing, accompanied by having to check for information leaks or other stages of data preprocessing by the a CNN model utilising DenseNet 121 framework, are thoroughly carried out now to train a model. Finally, the model is evaluated through ROC curve and visualised and analysed through GradCAM.

## VII. ACKNOWLEDGMENT

We would like to acknowledge Department of Biomedical Engineering and Department of Physics for their support and guidance.

## REFERENCES

- [1] W. H. Organization, "Cancer," 2018. [Online]. Available: <http://www.who.int/mediacentre/factsheets/fs297/en/>
- [2] C. Zwirowich, S. Vedal, R. R Miller, and N. L Mller, "Solitary pulmonary nodule: high-resolution ct and radiologic-pathologic correlation," vol. 179, pp. 469–76, 06 1991.
- [3] W. D. Jenkins, A. K. Matthews, A. Bailey, W. E. Zahnd, K. S. Watson, G. Mueller-Luckey, Y. Molina, D. Crumly, and J. Patera, "Rural areas are disproportionately impacted by smoking and lung cancer," *Preventive Medicine Reports*, vol. 10, pp. 200 – 203, 2018. [Online]. Available: <http://www.sciencedirect.com/science/article/pii/S2211335518300494>
- [4] T. Kubo, Y. Ohno, D. Takenaka, M. Nishino, S. Gautam, K. Sugimura, H. U. Kauczor, and H. Hatabu, "Standard-dose vs. low-dose ct protocols in the evaluation of localized lung lesions: Capability for lesion characterization lead study," *European Journal of Radiology Open*, vol. 3, pp. 67 – 73, 2016. [Online]. Available: <http://www.sciencedirect.com/science/article/pii/S2352047716300077>
- [5] Y. Lecun, L. Bottou, Y. Bengio, and P. Haffner, "Gradient-based learning applied to document recognition," *Proceedings of the IEEE*, vol. 86, no. 11, pp. 2278–2324, Nov 1998.
- [6] A. Krizhevsky, I. Sutskever, and G. E. Hinton, "Imagenet classification with deep convolutional neural networks," pp. 1097–1105, 2012.
- [7] M. D. Zeiler and R. Fergus, "Visualizing and understanding convolutional networks," in *Computer Vision – ECCV 2014*, D. Fleet, T. Pajdla, B. Schiele, and T. Tuytelaars, Eds. Cham: Springer International Publishing, 2014, pp. 818–833.
- [8] K. Simonyan and A. Zisserman, "Very deep convolutional networks for large-scale image recognition," vol. abs/1409.1556, 2014. [Online]. Available: <http://arxiv.org/abs/1409.1556>
- [9] C. Szegedy, W. Liu, Y. Jia, P. Sermanet, S. Reed, D. Anguelov, D. Erhan, V. Vanhoucke, and A. Rabinovich, "Going deeper with convolutions," in *2015 IEEE Conference on Computer Vision and Pattern Recognition (CVPR)*, vol. 00, June 2015, pp. 1–9. [Online]. Available: [doi.ieeecomputersociety.org/10.1109/CVPR.2015.7298594](https://doi.ieeecomputersociety.org/10.1109/CVPR.2015.7298594)
- [10] C. Szegedy, V. Vanhoucke, S. Ioffe, J. Shlens, and Z. Wojna, "Rethinking the inception architecture for computer vision," in *2016 IEEE Conference on Computer Vision and Pattern Recognition (CVPR)*, June 2016, pp. 2818–2826.
- [11] K. He, X. Zhang, S. Ren, and J. Sun, "Deep residual learning for image recognition," *2016 IEEE Conference on Computer Vision and Pattern Recognition (CVPR)*, pp. 770–778, 2016.
- [12] C. Szegedy, S. Ioffe, V. Vanhoucke, and A. A. Alemi, "Inception-v4, inception-resnet and the impact of residual connections on learning," in *AAAI*, 2017.
- [13] F. Chollet, "Xception: Deep learning with depthwise separable convolutions," *2017 IEEE Conference on Computer Vision and Pattern Recognition (CVPR)*, pp. 1800–1807, 2017.
- [14] G. Huang, Z. Liu, L. v. d. Maaten, and K. Q. Weinberger, "Densely connected convolutional networks," in *2017 IEEE Conference on Computer Vision and Pattern Recognition (CVPR)*, July 2017, pp. 2261–2269.
- [15] B. Zoph, V. Vasudevan, J. Shlens, and Q. V. Le, "Learning transferable architectures for scalable image recognition," vol. abs/1707.07012, 2017. [Online]. Available: <http://arxiv.org/abs/1707.07012>
- [16] M. T. Islam, M. A. Aowal, A. T. Minhaz, and K. Ashraf, "Abnormality detection and localization in chest x-rays using deep convolutional neural networks," vol. abs/1705.09850, 2017. [Online]. Available: <http://arxiv.org/abs/1705.09850>
- [17] X. Wang, Y. Peng, L. Lu, Z. Lu, M. Bagheri, and R. M. Summers, "Chestx-ray8: Hospital-scale chest x-ray database and benchmarks on weakly-supervised classification and localization of common thorax diseases," in *The IEEE Conference on Computer Vision and Pattern Recognition (CVPR)*, July 2017.
- [18] P. Rajpurkar, J. Irvin, K. Zhu, B. Yang, H. Mehta, T. Duan, D. Ding, A. Bagul, C. Langlotz, K. Shpanskaya, M. P. Lungren, and A. Y. Ng, "Chexnet: Radiologist-level pneumonia detection on chest x-rays with deep learning," vol. abs/1711.05225, 2017. [Online]. Available: <http://arxiv.org/abs/1711.05225>
- [19] Q. Guan, Y. Huang, Z. Zhong, Z. Zheng, L. Zheng, and Y. Yang, "Diagnose like a radiologist: Attention guided convolutional neural network for thorax disease classification," vol. abs/1801.09927, 2018. [Online]. Available: <http://arxiv.org/abs/1801.09927>
- [20] Jiuxiang Gu, Zhenhua Wang, Jason Kuen, Lianyang Ma, Amir Shahroudy, Bing Shuai, Ting Liu, Xingxing Wang, Gang Wang, Jianfei Cai, Tsuhan Chen, Recent advances in convolutional neural networks, *Pattern Recognition*, Volume 77, 2018, Pages 354–377, ISSN 00313203, <https://doi.org/10.1016/j.patcog.2017.10.013>.

- [21] WAN, Ji; WANG, Dayong; HOI, Steven C. H.; WU, Pengcheng; ZHU, Jianke; ZHANG, Yongdong; and LI, Jintao. Deep learning for contentbased image retrieval: A comprehensive study. (2014). MM '14: Proceedings of the 22nd ACM International Conference on Multimedia: November 3-7, 2014, Orlando. 157-166.
- [22] K. Simonyan and A. Zisserman "Very Deep Convolutional Networks for Large-Scale Image Recognition", in International Conference on Learning Representations 2015
- [23] Kingma, Diederik& Ba, Jimmy. "Adam: A Method for Stochastic Optimization". International Conference on Learning Representations. (2014)
- [24] Li. Deng and D. Yu, "Deep Learning," Signal Processing, vol. 7, pp. 34, 2014.
- [25] X. Glorot and Y. Bengio, "Understanding the difficulty of training deep feedforward neural networks," in Aistats, 2010, pp. 249-256.
- [26] M. Anthopoulos, S. Christodoulidis, L. Ebner, A. Christe, and S. Mougiakakou, "Lung Pattern Classification for Interstitial Lung Diseases Using a Deep Convolutional Neural Network," in IEEE Transactions on Medical Imaging, vol. 35, no. 5, pp. 1207-1216, May 2016. doi: 10.1109/TMI.2016.253 5865
- [27] G. van Tulder and M. de Bruijne, "Combining Generative and Discriminative Representation Learning for Lung CT Analysis With Convolutional Restricted Boltzmann Machines," IEEE transactions on medical imaging, vol. 35, no. 5, pp. 1262-1272, 2016.
- [28] P. Moeskops et al., "Automatic segmentation of MR brain images with a convolutional neural network," IEEE transactions on medical imaging, vol. 35, no. 5, pp. 1252-1261, 2016.
- [29] Z. Yan et al., "Multi-Instance Deep Learning: Discover Discriminative Local Anatomies for Bodypart Recognition," IEEE transactions on medical imaging, vol. 35, no. 5, pp. 1332-1343, 2016.
- [30] Y. Lecun, L. Bottou, Y. Bengio and P. Haffner, "Gradient-based learning applied to document recognition," in Proceedings of the IEEE, vol. 86, no. 11, pp. 2278-2324, Nov 1998
- [31] X. Wang, Y. Peng, L. Lu, Z. Lu, M. Bagheri and R. M. Summers, "ChestX-Ray8: Hospital-Scale Chest X-Ray Database and Benchmarks on Weakly-Supervised Classification and Localization of Common Thorax Diseases," 2017 IEEE Conference on Computer Vision and Pattern Recognition (CVPR), 2017, pp. 3462-3471, doi: 10.1109/CVPR.2017.369.
- [32] O. Russakovsky, J. Deng, H. Su, J. Krause, S. Satheesh, S. Ma, Z. Huang, A. Karpathy, A. Khosla, M. S. Bernstein, A. C. Berg, and F. Li, "Imagenet large scale visual recognition challenge," vol. abs/1409.0575, 2014. [Online]. Available: <http://arxiv.org/abs/1409.0575>

